

Eternal Inflation, Bubble Collisions, and the Disintegration of the Persistence of Memory

Ben Freivogel¹, Matthew Kleban², Alberto Nicolis³, and Kris Sigurdson⁴

¹ *Berkeley Center for Theoretical Physics, Department of Physics
University of California, Berkeley, CA 94720-7300, USA*

and

Lawrence Berkeley National Laboratory, Berkeley, CA 94720-8162, USA

² *Center for Cosmology and Particle Physics,
Department of Physics, New York University,
4 Washington Place, New York, NY 10003, USA*

³ *Department of Physics and ISCAP,
Columbia University, New York, NY 10027, USA*

⁴ *Department of Physics and Astronomy,
University of British Columbia, Vancouver, BC V6T 1Z1, Canada*

Abstract

We compute the probability distribution for bubble collisions in an inflating false vacuum which decays by bubble nucleation. Our analysis generalizes previous work of Guth, Garriga, and Vilenkin to the case of general cosmological evolution inside the bubble, and takes into account the dynamics of the domain walls that form between the colliding bubbles. We find that incorporating these effects changes the results dramatically: the total expected number of bubble collisions in the past lightcone of a typical observer is $N \sim \gamma V_f/V_i$, where γ is the fastest decay rate of the false vacuum, V_f is its vacuum energy, and V_i is the vacuum energy during inflation inside the bubble. This number can be large in realistic models without tuning. In addition, we calculate the angular position and size distribution of the collisions on the cosmic microwave background sky, and demonstrate that the number of bubbles of observable angular size is $N_{LS} \sim \sqrt{\Omega_k} N$, where Ω_k is the curvature contribution to the total density at the time of observation. The distribution is almost exactly isotropic.

¹e-mail: freivogel@berkeley.edu

²e-mail: mk161@nyu.edu

³e-mail: nicolis@phys.columbia.edu

⁴e-mail: krs@phas.ubc.ca



Figure 1: *The Persistence of Memory*, Salvador Dalí, 1931

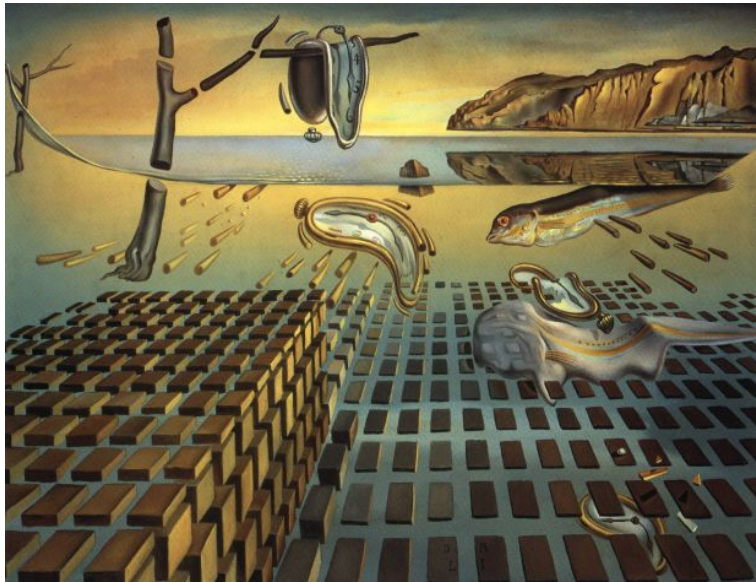


Figure 2: *The Disintegration of the Persistence of Memory*, Salvador Dalí, c. 1952-1954.

“My father today is Dr. Heisenberg” -Salvador Dalí, *Anti-Matter Manifesto*, 1958

1 Introduction

In a model like the string theory landscape [1, 2] one may expect our observable universe to be contained inside a bubble which is surrounded by an eternally inflating false vacuum. Quantum tunneling and thermal effects allow the false vacuum to decay, producing regions of lower energy—like the one we inhabit—which expand and may themselves decay in turn. If the decay rate of the false vacuum in Hubble units is less than a particular order one number, this process never terminates. The false vacuum produces new volume through exponential expansion faster than it loses volume due to decays.

Nevertheless any bubble will collide with many others, forming a cluster that grows without bound as time passes, as first described in [3]. We would like to ask whether observers like ourselves can expect to have a bubble collision in our past. If the answer is yes, then we would like to know the expected number of collisions, their distribution in size and direction, and their observable consequences.

This distribution of vacuum bubble collisions was analyzed recently in a very interesting paper [4] by Guth, Garriga, and Vilenkin (GGV) titled “Eternal inflation, bubble collisions, and the persistence of memory.” The analysis of GGV was done in the approximation that the cosmological constant inside the observation bubble is the same as the cosmological constant of the false vacuum. Also, GGV assumed that observers cannot form anywhere in the future lightcone of collisions.

With these assumptions, GGV computed the probability distribution for bubble collisions which may become visible in the future. They found that a typical observer inside such a bubble sees an anisotropic distribution of collisions. The anisotropy is left over from the initial conditions, and does not go away even in the limit that the observation bubble nucleates an infinitely long time after the initial conditions. They called this lingering effect of the initial conditions “the persistence of memory.”

However they also found that the overall rate at which an observer sees collisions (and the probability of observing any collisions) is proportional to the dimensionless decay rate γ of the false vacuum, a quantity that is typically exponentially small. Moreover they found that the typical distance to the nearest collision is large, of order $-\ln \gamma$ in units of curvature radius.

In this note we consider the case relevant for observation, where the interior of the observation bubble is similar to our universe. We assume that due to the dynamics of the domain walls, collisions disrupt structure formation in only part of their future lightcone (as described in more detail in section 2.1). We find that these changes have a major impact on the result. The ratio of the vacuum energy in the false vacuum to the inflationary vacuum energy, V_f/V_i , which was set to one in the GGV approximation, can be large in realistic scenarios. Among other things, this ratio turns out to divide the anisotropic term in the distribution and multiply the expected number of bubbles in the past lightcone of a late-time observer. Incorporating the effects of domain walls renders the distribution smooth and finite even for observers at infinite “boost”.

A heuristic argument for the distribution of bubbles in our past lightcone is as follows.

In the inflating false vacuum there is an event horizon with radius of $R_f = H_f^{-1}$ (where $H_f \sim \sqrt{\Lambda_f}$ is the false vacuum Hubble constant) surrounding every point. This horizon shields the bubble from interacting with any event (such as another bubble's nucleation) that occurs more than a distance H_f^{-1} away from its walls. Hence the bubble wall is surrounded at all times by a shell H_f^{-1} thick inside of which any bubble nucleation leads to a collision. As the bubble grows the volume of this region expands like its surface area, and at the same time the relative size of the late-appearing bubbles shrinks. This leads to a size distribution of bubble collisions which, as a function of angular radius on the fiducial bubble, increases rapidly with decreasing size. Further, as bubble grows the initial conditions become unimportant, so the anisotropy is insignificant for small bubbles.

To compute the total number of bubbles, we need to know the 4-volume in the false vacuum available to nucleate bubbles that will collide with our own. The surface area of the bubble wall inside the past lightcone of late-time observers like us is of order H_i^{-2} , where H_i is the Hubble constant during slow-roll inflation inside the bubble. As mentioned above, the distance from the bubble wall to the event horizon is H_f^{-1} . To get the 4-volume, we just need to know the amount of time available for creating collision bubbles, which turns out to also be given by H_f^{-1} .

As a result the 4-volume of the false vacuum available for bubble nucleations scales as $H_f^{-2}H_i^{-2}$. If Γ is the decay rate per 4-volume, the total number of bubbles in our past lightcone is $N \sim \Gamma H_i^{-2}H_f^{-2}$. Defining the dimensionless decay rate $\gamma \equiv \Gamma H_f^{-4}$, we have

$$N \sim \gamma \left(\frac{H_f}{H_i} \right)^2 . \quad (1.1)$$

It is crucial in deriving this answer that observers can form in a reasonable fraction of the future lightcone of the collision. Whether this is true depends primarily on the dynamics of the domain wall that is formed in the collision. The domain wall will have constant proper acceleration and approach the speed of light. Depending on parameters it may accelerate into our bubble or away from our bubble.

If the domain wall accelerates into our bubble, then most of the future lightcone of a collision is uninhabitable because it is eaten by the collision bubble, and the probability of observing a collision will be small, as in GGv. Further, such an observation would be followed nearly instantaneously by a fatal collision with the domain wall.

We choose to analyze the more optimistic case where the domain wall formed in the collision accelerates away from our bubble. As we describe in section 2.1, it is reasonable to expect that in this case an order one fraction of the future lightcone of the collision is inhabitable, and the estimate (1.1) holds.

Finally, one could also analyze the case where our bubble collides with identical bubbles. In this case no domain wall forms after the collision, and again we expect an order one fraction of its future lightcone to be inhabitable. We will focus on the case where the collision produces a domain wall, but we expect that our analysis carries over almost unchanged to the collision of our bubble with identical bubbles.

1.1 Results

Our primary result is that the expected number of bubble collisions in our past is

$$N \approx \frac{4\pi}{3} \gamma \left(\frac{H_f}{H_i} \right)^2 . \quad (1.2)$$

Here $\gamma \sim e^{-S}$ is the dimensionless decay rate of the false vacuum to its fastest decay product. The inflationary Hubble scale H_i is very poorly constrained, but assuming the vacuum energy in the false vacuum is of order the Planck scale, observational bounds on tensor modes imply that $(H_f/H_i)^2 \gtrsim 10^{12}$, and it can be larger than 10^{80} in models of low scale inflation. Also, the decay rate is bounded below by the recurrence time of the false vacuum de Sitter space, $\gamma > \exp(-S_f)$ with $S_f \sim (M_P/H_f)^2$. If the vacuum energy of the false vacuum is near the Planck scale the decay rate cannot be too small. So even though bubble nucleation is exponentially suppressed, the total number of bubbles in the past lightcone of a typical observer can be large with no fine-tuning.

We derive the distribution of bubble collisions in the backward lightcone of a single observer as a function of the angular coordinates θ and ϕ of the center of the collision bubble, a parameter \mathcal{X} that controls the center of mass energy of the collision, and the conformal time η_v when the collision first becomes visible (**Eq. 2.9**).

We find that the ‘‘persistence of memory’’ effect discovered by GGv is significantly modified when the vacuum energy during inflation is allowed to be different from the cosmological constant of the false vacuum. The memory of the initial conditions, which manifests itself as an anisotropy in the angular distribution, disappears in the limit that the bubble has small cosmological constant inside (**Eqs. 2.9 and C.23**) and the late-time distribution becomes precisely boost and rotationally invariant around the bubble’s nucleation point (**Eq. B.39**).

Finally, we derive the distribution of collision lightcones on the last scattering surface as a function of their position and angular size on the CMB sky (**Eq. 4.25**). Bubbles that collide with ours very early have lightcones that completely cover the part of the last scattering surface we can see, and these are probably not observable in the limit that the size of the region they cover is much greater than the observable part. But bubble collisions that occurred somewhat later have lightcones that bisect the observable part of the last scattering surface (and hence the CMB sky), and these can directly affect the cosmic microwave background temperature map and are of observational interest. The total number of such bubbles is

$$N_{LS} \approx 4\zeta_0 N \sqrt{\Omega_k} = \frac{16\pi}{3} \zeta_0 \gamma \left(\frac{H_f}{H_i} \right)^2 \sqrt{\Omega_k} . \quad (1.3)$$

where $\zeta_0 \approx 10/3$ is a constant that depends upon the cosmological evolution inside the bubble after reheating (see Appendix D for details) and Ω_k is the curvature contribution to Ω_{tot} .

1.2 Related work

Our work is closely related to the analysis of Aguirre, Johnson, and collaborators [5, 6, 7], with the crucial difference that we treat the effects of bubble collisions on observer formation

in a different (and in our opinion more realistic) way. Our results are in rough agreement with [5] for the number and distribution of “small” bubbles, where “small” here means bubbles that are smaller than the observation bubble in the observer’s reference frame. The number of such bubbles was computed in [5] and their isotropy was noted by [5] and [8]. However because of our assumptions about the disruptive effects of collisions on observer formation, our results for the distribution of large bubbles and our conclusions for the potential observability of collisions differ sharply from [5, 6, 7].

Ref. [5] focused on the case where bubble collisions have approximately no effect on observer formation, and found that typical observers see an arbitrarily large number of very large, anisotropically distributed bubbles. The infinity is removed here by our treatment of the domain walls. Ref. [7] did a numerical analysis of a single collision and found that the region far to the future of the resulting domain wall has an approximate $SO(3, 1)$ invariance restored (similar to the case of a single bubble without a collision), which may remain if no other decays or collisions take place to perturb it. Based on this and on the conclusions of GGv, [7] concluded that the fraction of observers that can see a collision is very small. However, even under this set of assumptions computing this fraction unambiguously is difficult, as it requires comparing two infinite volume regions.

After this work was completed and while the manuscript was in preparation we received Ref. [9], which concluded that the fraction of observers that see collisions can be $\mathcal{O}(1)$, but performed the analysis in the approximation that the domain walls between bubbles do not accelerate and that the observation and collision bubbles are identical and dominated by vacuum energy inside. In this work we will take the acceleration of the domain walls into account and allow for a fully realistic cosmology inside the observation bubble.

The motion of the post-collision domain walls was studied in [10] and [11] in special cases, and then more generally in [12] and [6].

Determining the observational consequences for observers in the space to the future of a bubble collision is a rich problem that has been addressed by [5, 6, 7] and by [12, 13]. In particular [13] studied in detail the effects on the cosmic microwave background of collision lightcones that bisect the observable part of the last scattering surface.

2 Probability distribution for bubble collisions

We want to compute the probability distribution for bubbles that collide with our own. Before including other bubbles, the exterior of our bubble is in the false vacuum. We work in the approximation that the domain wall of our bubble is lightlike, and that the metric outside the lightcone is undisturbed de Sitter space with cosmological constant H_f^2 . This approximation does not have a large effect on our results, and going away from it would introduce new model-dependent parameters.

A convenient coordinate system that covers the region where collision bubbles can nucleate is

$$ds^2 = H_f^{-2} \frac{1}{\cosh^2 \mathcal{X}} (d\mathcal{X}^2 + dS_3^2) \quad (2.1)$$

where dS_3^2 is the metric of a unit 2 + 1 dimensional de Sitter space and H_f is the Hubble constant of the false vacuum. Boosts that leave the observation bubble fixed act as the full symmetry group of the 2 + 1 de Sitter space, while leaving \mathcal{X} fixed. Therefore collisions with different \mathcal{X} are physically different, while any two collisions with the same \mathcal{X} can be boosted into each other by acting with the symmetries.

Choosing coordinates on the de Sitter space, the metric is

$$ds^2 = H_f^{-2} \frac{1}{\cosh^2 \mathcal{X}} (d\mathcal{X}^2 - d\tau^2 + \cosh^2 \tau d\Omega_2^2) \quad (2.2)$$

where \mathcal{X} and τ run from $-\infty$ to ∞ . These coordinates cover the region outside our bubble that is capable of nucleating bubbles that will collide with our own. The nucleation point of our bubble is at $\mathcal{X} = -\infty$ and τ finite, while the domain wall of our bubble is the null surface $\mathcal{X} = -\infty$ with $\tau \geq 0$. The null surface $\mathcal{X} = \infty$ bounds the region where nucleated bubbles will collide with our bubble.

We are interested in observing bubble collisions from inside the bubble, while the coordinate system above covers the outside of the bubble. For the moment we leave the cosmological history general inside the bubble. Before considering the effects of collisions, the interior geometry has $SO(3, 1)$ symmetry. The metric can be written

$$ds^2 = a^2(\eta)(-d\eta^2 + d\rho^2 + \sinh^2 \rho d\Omega_2^2), \quad (2.3)$$

where without loss of generality we focus on an observer at $\rho = 0$. This metric describes a homogeneous and isotropic Robertson-Walker cosmology. An unperturbed observation bubble will inflate and reheat along slices of constant η , and comoving observers move on trajectories with fixed spatial coordinates¹.

This metric is smooth all the way down to the “big bang” $\eta = -\infty$, even though $a(\eta) \rightarrow 0$ there. The reason for this non-singular “big bang” is that the instanton boundary conditions require [14]

$$a(\eta) \approx \frac{2}{H_f} e^\eta + \mathcal{O}(e^{3\eta}) \quad \text{as } \eta \rightarrow -\infty \quad (2.4)$$

where the multiplicative factor $2/H_f$ is arbitrary and has been chosen for convenience. For example if one follows the past lightcone $\rho + \eta = \eta_0$ of an observer at time η_0 , the radius of the bubble lightcone is $a(\eta) \sinh(\rho) \rightarrow e^{\eta+\rho}/H_f = e^{\eta_0}/H_f$, which is finite as $\eta \rightarrow -\infty$ and $\rho \rightarrow \infty$.

Consider a bubble that nucleates at a point $(\mathcal{X}, \tau, \theta, \phi)$. The collision occurs along a spacelike hyperboloid that preserves $SO(2, 1)$ symmetry, as shown in figure 3. The bubble will appear as some type of disturbance on the observer’s sky. The angular location of the center of the disturbance is given by the angular location (θ, ϕ) of the bubble nucleation. We would like to compute the time at which the collision first enters the backward lightcone of the observer at $\rho = 0$. Ingoing radial null rays satisfy $\mathcal{X} + \tau = c$ outside the bubble and

¹Note that we are using conventions where the scale factor a has units of length, and the spatial curvature is $k = -1$.

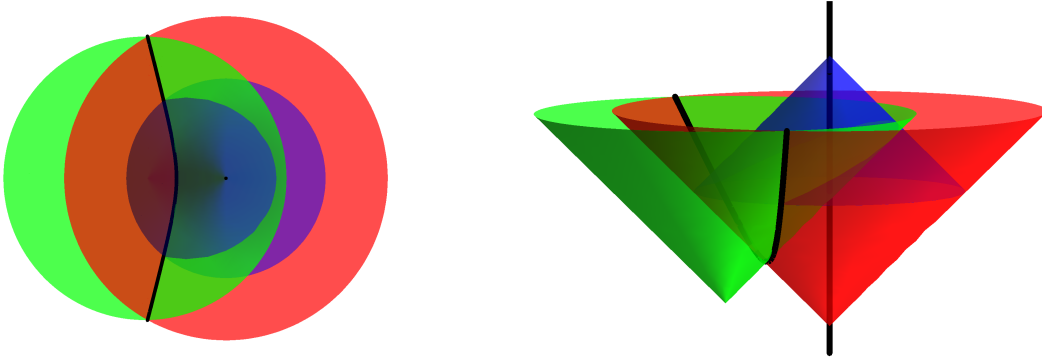


Figure 3: Two views of the collision of two bubbles in spacetime. The red cone is the observation bubble lightcone, the green cone is the collision bubble lightcone, the straight black line is the worldline of the observer, and the hyperbolic black line is the surface along which the bubbles collide. The angular size of the collision as seen by the observer at some time is determined by the intersection of the observer's past lightcone (in blue) with the observation bubble wall, or with the surface of last scattering.

(with our choice of coordinates) $\eta + \rho = c$ inside the bubble, where c is an arbitrary constant. So the future lightcone of a bubble nucleated at (\mathcal{X}, τ) first reaches $\rho = 0$ at the conformal time

$$\eta_v = \mathcal{X} + \tau. \quad (2.5)$$

A given collision is described by four parameters: two angular coordinates (θ, ϕ) give the angular location of the center of the collision, η_v is the time when the collision first becomes visible, and \mathcal{X} sets the intrinsic properties of the collision. For example, the radius of curvature of the collision hyperboloid is $r_c = \exp(\mathcal{X})$.

The probability to nucleate a bubble in an infinitesimal region is proportional to the 4-volume of that region,

$$dN = \gamma H_f^4 dV_4, \quad (2.6)$$

where γ is the dimensionless nucleation rate. The infinitesimal 4-volume in our coordinates (2.2) is

$$dV_4 = H_f^{-4} \frac{d\mathcal{X}}{\cosh^4 \mathcal{X}} \cosh^2 \tau d\tau d^2\Omega_2. \quad (2.7)$$

We can exchange the coordinate τ for the conformal time η_v at which the collision enters the backward lightcone by using (2.5). So the naive probability distribution for collisions is

$$dN = \gamma \frac{\cosh^2(\eta_v - \mathcal{X})}{\cosh^4 \mathcal{X}} d\eta_v d\tau d^2\Omega_2 \quad (2.8)$$

Again naively, the total number of collisions visible to an observer at conformal time η_0 is given by integrating the above equation over the entire range of parameters, subject to the constraint $\eta_v < \eta_0$. However this integral diverges at $\eta_v \rightarrow -\infty$, corresponding to an infinite probability to have nucleated a bubble in the arbitrarily far past.

There are several reasons the above analysis is naive, which is fortunate since the answer is infinite. We discuss various corrections throughout the rest of the paper.

2.1 Disruptive effects of collisions

The most important correction is that bubble collisions will disrupt structure formation in some part of their future lightcone. Since we are interested in making a prediction for our observations, we need to compute the distribution of bubble collisions *consistent with the presence of observers*. We show in this subsection that this requirement regulates the infinity of the naive analysis and allows for a well-defined prediction for the distribution of bubbles..

The collision can disrupt structure formation throughout its future lightcone, but it is reasonable to expect that in some regions the bubble collision has a small effect, while in other regions no structure forms. We focus on the collision of our bubble with some other type of bubble, so that a domain wall forms in the collision. Vacuum energies and domain wall tensions are generically Planckian in the landscape, so we assume that both the false vacuum and the collision bubble have Planckian vacuum energy, and that the domain walls in the problem also have Planckian tension. The vacuum energy in the collision bubble could be negative or positive.

We make the approximation that structure formation occurs unchanged in the observation bubble, except that the domain wall with the collision bubble removes regions that otherwise would have formed structure. Because the vacuum energy in the collision bubble is Planckian, no observers can form in the collision bubble.

The key question is regarding the dynamics of the domain wall. Because we have assumed that the vacuum energy of the collision bubble and the tension of the domain wall are Planckian, the acceleration of the domain wall is generically Planckian. But the domain wall may accelerate into the observation bubble, or away from the observation bubble. In either case the domain wall undergoes constant proper acceleration and asymptotically approaches the speed of light.

If the domain wall accelerates into the observation bubble, then nearly all of the future lightcone of the collision is behind the domain wall, and since we have assumed that observers can only form in the observation bubble there are essentially zero observers in the future lightcone of the collision.

If the domain wall accelerates away from the observation bubble, then some observers will form in the future lightcone of the collision. We focus on this case. If the vacuum energy of the collision bubble is positive, then it is guaranteed that the domain wall accelerates away from the observation bubble. If the vacuum energy of the collision bubble is negative, then the acceleration of the domain wall depends on the tension; for sufficiently large tension the domain wall again accelerates away from the observation bubble.

The detailed dynamics of the domain wall are somewhat involved and model-dependent [10, 11, 12, 6], but with our assumptions Planckian acceleration is generic. The initial velocity of the domain wall after the collision is also model dependent, but typically it will take some time for the messy collision to settle down into a coherent domain wall; with our assumptions this time scale is also Planckian. In order to have some control over our calculation we assume that the energy scales are all somewhat less than Planckian, and instead set by the outside Hubble constant H_f .²

Therefore, we adopt the following caricature of the domain wall motion: we assume the domain wall moves into the observation bubble at the speed of light for a time H_f^{-1} . Then it turns around and moves outward at the speed of light. While this approximation could certainly be improved upon in specific models, it captures the crucial physics of the problem.

As discussed in the paragraph below Eq. 2.3, the metric has a coordinate singularity $a \rightarrow 0$ as $\eta \rightarrow -\infty$. With our choice of coordinates $\eta = 0$ corresponds to a time of order H_f^{-1} . Therefore we will approximate the domain wall trajectory as null and ingoing for $\eta < 0$, null and outgoing for $\eta > 0$. Bubbles whose domain walls cover $\rho = 0$ at any time during their evolution are assumed to disrupt reheating. Therefore, given our assumptions, we prohibit bubbles with $\eta_v < 0$.

2.2 Summary

Now we can compute the distribution of bubbles that are in the backward lightcone of an observer at the conformal time η_0 . It is

$$dN = \gamma \frac{\cosh^2(\eta_v - \mathcal{X})}{\cosh^4 \mathcal{X}} d\mathcal{X} d\eta_v d^2\Omega_2 \quad (2.9)$$

$$0 < \eta_v < \eta_0 \quad (2.10)$$

where the restriction $0 < \eta_v$ comes from requiring the observer formation is not disrupted.

We can integrate out \mathcal{X} to get the distribution as a function of conformal time,

$$dN = \frac{2\gamma}{3} (1 + 2 \cosh 2\eta_v) d\eta_v d^2\Omega_2 \quad \text{for } \eta_v > 0 \quad (2.11)$$

Integrating, the total number of collisions visible before some conformal time η_0 is

$$N(\eta_0) = \frac{8\pi\gamma}{3} (\sinh 2\eta_0 + \eta_0) . \quad (2.12)$$

There is an important subtle point that we have glossed over here. The divergence present in the naive distribution means that the probability of observer formation at $\rho = 0$ is zero. Therefore, one could ask whether the above distribution is meaningful. The answer is that any choice of initial conditions will regulate the infinity so that the probability of observer formation is finite. Further, the actual choice of initial conditions will have little effect on the distribution, so that the net effect is simply that we can take the above equations seriously.

²In fact, the typical energy scale associated with the vacuum energy, the tension of the wall, and its acceleration, is the geometric mean between the Planck scale and H_f . In the following we will ignore this point, for it does not lead to any substantial modification of our results.

3 Effect of the initial condition surface: how persistent is memory?

Because the false vacuum is only metastable, it is not consistent to imagine that it exists eternally. To have a well-defined Cauchy problem, one needs to choose an initial condition on a spacelike or null surface. An obvious (but ad hoc) choice is to put the fields in a false-vacuum minimum on some slice of constant de Sitter time and then consider the forward time evolution. One of the surprising results of the work of [4] was that observers inside bubbles that form to the future of this initial condition surface always retain some memory of it no matter how far in the future they live, in the sense that the angular distribution of incoming bubbles remains significantly anisotropic except for the special single observer in the case of an isotropic initial condition surface who sees an isotropic distribution. We will see that incorporating a realistic cosmology inside the bubble in the analysis alters this conclusion significantly.

For an initial condition we follow [4] in taking the surface to be $t = -\infty$ in the standard de Sitter flat slicing. This choice has the advantage that it is infinitely far back in the past, but still regulates the divergence in Eq. (2.7). On the other hand, [4] found that with this choice only a single special observer co-moving inside the observation bubble will see an isotropic distribution, because generic co-moving observers are boosted with respect to the flat slicing.

For this discussion, since we are interested in comparing different observers related by boosts around the nucleation point of the bubble, it will be helpful to use the embedding coordinates for de Sitter space in which all of the symmetries are manifest. 3 + 1 dimensional de Sitter space can be embedded in 4 + 1 dimensional Minkowski space as the surface

$$X^2 + R^2 - T^2 = 1 \tag{3.1}$$

where $R^2 = Y^2 + Z^2 + W^2$ and we have set

$$H_f = 1 \text{ in this section.} \tag{3.2}$$

The initial condition surface in embedding coordinates is $X + T = 0$.

The relation to the parameters of the bubble collision is

$$\begin{aligned} T &= \frac{\sinh \tau}{\cosh \mathcal{X}} \\ X &= -\tanh \mathcal{X} \\ Y &= \frac{\cosh \tau}{\cosh \mathcal{X}} \cos \theta \\ Z &= \frac{\cosh \tau}{\cosh \mathcal{X}} \sin \theta \cos \phi \\ W &= \frac{\cosh \tau}{\cosh \mathcal{X}} \sin \theta \sin \phi \end{aligned}$$

where we have chosen the observation bubble to nucleate at $X = 1, T = Y = Z = W = 0$. Recall that the coordinate τ is related to our preferred parameter η_v by $\eta_v = \tau + \mathcal{X}$.

With this choice for the initial condition surface, allowed collision bubbles nucleate in the region $X + T > 0$. Translating to the parameters of the bubble collision, this condition is

$$-\tanh \mathcal{X} + \frac{\sinh \tau}{\cosh \mathcal{X}} > 0, \quad (3.3)$$

which is equivalent to

$$\mathcal{X} < \tau. \quad (3.4)$$

This is the appropriate condition for the special “unboosted” observer (the observer that is comoving in the bubble and at rest in the flat slicing). To consider boosted observers, we can simply boost the initial condition surface. The boost should preserve the nucleation point of the observation bubble; consider without loss of generality a boost in the YT plane. The boosted initial condition surface is

$$X + T \cosh \xi + Y \sinh \xi > 0 \quad (3.5)$$

where ξ parameterizes the boost. In our coordinates this condition becomes

$$\sinh \mathcal{X} < \sinh \tau \cosh \xi + \cosh \tau \sinh \xi \cos \theta. \quad (3.6)$$

The 4-volume available for bubble nucleations is restricted by the above inequality.

Now the initial condition surface is ambiguous, because we do not know our boost ξ . However, we will show that the expected number of bubbles that satisfy the other constraints but are prohibited by the initial condition surface is generally much less than one! Therefore, the unknown parameter ξ has a small effect on the final distribution.

To show this, we will compute the total number of collisions in the past lightcone of an observer in a cosmology like ours that are allowed by the other constraints but prohibited by the initial condition surface. The answer for arbitrary ξ is easy to calculate but is slightly complex, so we will just present the answer at zero and infinite boost.

At zero boost the initial condition surface imposes $\mathcal{X} < \tau$, so the expected number of bubbles that are allowed by the other constraints but prohibited by the initial conditions surface is

$$\Delta N(\xi = 0) = \gamma \int d\mathcal{X} \int d\tau \int d^2\Omega \frac{\cosh^2 \tau}{\cosh^4 \mathcal{X}} \quad (3.7)$$

integrated over the region

$$0 < \mathcal{X} + \tau < \eta_0 \quad \mathcal{X} > \tau \quad (3.8)$$

Evaluating this integral gives $\Delta N(\xi = 0) = (4\pi\gamma/3)(1 + \ln 4) + \mathcal{O}(\gamma e^{-\eta_0})$.

At infinite boost, the initial condition surface requires $\cos \theta + \tanh \tau > 0$. Performing the integral, the number of bubbles prohibited by the initial condition surface only is $\Delta N(\xi = \infty) = (4\pi\gamma/3)(\eta_0 + 1) + \mathcal{O}(\gamma e^{-\eta_0})$.

We will show in the next section that the conformal time η_0 for an observer like us is approximately

$$\eta_0 \approx \log \frac{H_f}{H_i} \quad (3.9)$$

where H_i is the Hubble constant during slow roll inflation. Since one expects γ to be exponentially small, generically $\Delta N(\xi) \ll 1 \quad \forall \xi$.

4 Observability of Collisions

In this section we will use this result to determine the total number of collisions that are potentially detectable by an observer in a realistic cosmology.

4.1 Computation of the conformal time

To justify our claim that $\eta_0 \approx \log \frac{H_f}{H_i}$, we need to relate η to the proper time of a comoving observer in the observation bubble. The conformal time η is related to the observer's proper time t by $d\eta = dt/a(t)$. The constant of integration is fixed by demanding that

$$a(\eta) \rightarrow \frac{1}{2H_f} e^\eta \quad \text{as } \eta \rightarrow -\infty \quad (4.1)$$

as mentioned in the discussion below Eq. (2.3).

To proceed we will need an explicit form for $a(t)$. Approximating slow-roll inflation by de Sitter space with Hubble constant H_i , $a(t) = H_i^{-1} \sinh(H_i t)$ for $t < t_e$. During this time, the scale factor as a function of conformal time is

$$a^2(\eta) = \frac{H_i^{-2}}{\sinh^2(\eta - \log \frac{H_f}{H_i})} \quad (4.2)$$

where the additive constant in η is fixed by the convention (4.1).

Defining the number N of efoldings by $a_{RH} \equiv H_i^{-1} e^N$, the conformal time at reheating is

$$\eta_{RH} = \log \frac{H_f}{H_i} - e^{-N} \approx \log \frac{H_f}{H_i} \quad (4.3)$$

for $a_{RH} \gg H_i^{-1}$.

After reheating, the behavior of the scale factor depends upon which type of matter or energy is dominating the expansion of the Universe at a particular epoch. It is approximately $a(t) = H_i^{-1} e^N (t/t_{RH})^p$, where $p = 1/2$ or $2/3$ for radiation or matter domination respectively. Eventually a will asymptote to t (if there were no dark energy) or to an exponential if there is a cosmological constant in the bubble. We consider in detail the realistic case with arbitrary matter, radiation, curvature, and cosmological constant content in Appendix D. Here, we illustrate the calculation for the simpler case where the scale factor is a power law of the cosmic time.

Taking $a(t) = H_i^{-1} e^N (t/t_{RH})^p$ and integrating, we get

$$\eta(t) - \eta_{RH} = \frac{1}{1-p} \left(\frac{t}{a(t)} - \frac{t_e}{a(t_e)} \right) \quad (4.4)$$

For times much later than reheating, and many efoldings of inflation, this is

$$\eta(t) = \log \frac{H_f}{H_i} + \frac{1}{1-p} \frac{t}{a(t)} \quad (4.5)$$

We would like to relate this to observable quantities. The ‘‘curvature contribution’’ to the total energy density is defined by

$$\Omega_k(t) \equiv \frac{1}{H^2 a^2} = \frac{1}{\dot{a}^2} \quad (4.6)$$

We have $\dot{a} = pa/t$ so the conformal time can be written

$$\eta(t) = \log \frac{H_f}{H_i} + \frac{p}{1-p} \sqrt{\Omega_k(t)} \quad (4.7)$$

Finally, most of the time (and most of the conformal time) since reheating is during matter domination, so setting $p = 2/3$ we have

$$\eta(t) \approx \log \frac{H_f}{H_i} + 2\sqrt{\Omega_k(t)} \quad (4.8)$$

valid for times well into matter domination and before dark energy or curvature domination. More generally we find that the expression for the conformal time today is

$$\eta_0 \approx \log \frac{H_f}{H_i} + \zeta_0 \sqrt{\Omega_k} \quad (4.9)$$

where $\zeta_0 \approx 3.3$ for allowed values of the cosmological parameters (see Appendix D).

The conformal time grows logarithmically with time for the first efold of inflation, rapidly asymptoting to $\log H_f/H_i$. After inflation it remains almost constant until late times, when— if the curvature becomes significant—it will begin to grow again. If our universe has a small positive vacuum energy and is nearly flat then curvature domination never occur and the effects of collisions weaken from the onset of cosmological constant domination onward, making the current cosmological era an opportune time to observe them [15].

The total number of collisions in a universe similar to ours at the present time t_0 will be

$$N \approx \frac{8\pi\gamma}{3} (\sinh 2\eta_0 + \eta_0) \approx \frac{4\pi\gamma}{3} \left[\left(\frac{H_f}{H_i} \right)^2 e^{2\zeta_0 \sqrt{\Omega_k(t)}} + 2 \log \frac{H_f}{H_i} + 2\zeta_0 \sqrt{\Omega_k(t)} \right]. \quad (4.10)$$

To compute the total number in our backward lightcone now, we use $\Omega_k(t_0) \ll 1$ and also expand for $H_f/H_i \gg 1$ to get

$$N \approx \frac{4\pi\gamma}{3} \left(\frac{H_f}{H_i} \right)^2 (1 + 2\zeta_0 \sqrt{\Omega_k} + \dots) \quad (4.11)$$

where the ... denotes terms which are much smaller than one. (See appendix C of [6] for a more detailed computation of this quantity.) The $\sqrt{\Omega_k}$ term is at most an order one multiplicative correction, so the bottom line is

$$N \approx \frac{4\pi\gamma}{3} \left(\frac{H_f}{H_i} \right)^2 \quad (4.12)$$

There is no reason to expect this number to be small. While one expects $\gamma \ll 1$, observational constraints require $(H_f/H_i)^2 \gtrsim 10^{12}$ if $H_f \sim M_{\text{Pl}}$. In models of low-scale inflation H_i can be very small; in such models the ratio $(H_f/H_i)^2$ can be 10^{80} or more. Moreover, the relevant γ is the fastest decay channel of the false vacuum around the observation bubble. In models like the string theory landscape, there are an enormous number of decay channels available. $\gamma < 1$ is required for our analysis to be valid, but it is not clear how much smaller than one we should expect it to be.

4.2 Distribution at Last Scattering

One of the most promising possibilities for observing these collisions comes from the cosmic microwave background. In order for a collision to make an observable mark on the CMB, the collision bubble lightcone should be of reasonable size when it intersects the part of the last scattering volume we can observe. If it is smaller than a fraction of a degree it will be lost in the noise, and if it is much larger than the observable part of the reheating volume the signal will be degenerate with the dipole from the peculiar velocity of the earth in the CMB rest frame [13]. However if it has an angular size of order one, it can create potentially observable disks on the CMB inside of which the average temperature is affected in an angle-dependent way [13]. Therefore the collisions of most interest observationally are those with lightcones that bisect the observable part of the last scattering volume.

We describe the bubbles first in terms of their comoving distance from $\rho = 0$ at last scattering. Then we will convert this to their angular size. For a collision which is not yet in the backward lightcone of $\rho = 0$ at last scattering, the shortest comoving distance to the lightcone is given by the part of the lightcone which travels radially,

$$\rho + \eta_{LS} = \eta_v \quad (4.13)$$

so that the comoving distance is

$$\ell(\eta_{LS}) = \eta_v - \eta_{LS} \quad (4.14)$$

For bubbles that are already in the backward lightcone of $\rho = 0$ at last scattering, ℓ is negative but its magnitude still gives the shortest comoving distance from $\rho = 0$ to the collision lightcone.

To summarize, we will trade in η_v , the time the future lightcone of the collision crosses $\rho = 0$, for ℓ , the comoving distance from $\rho = 0$ to the collision lightcone at last scattering. We allow ℓ to be positive or negative, with positive ℓ corresponding to collisions that have not yet crossed $\rho = 0$ at last scattering, and negative ℓ corresponding to collision that have already crossed $\rho = 0$.

Let's rewrite our distribution in terms of ℓ . We change variables in the distribution by substituting

$$\eta_v = \ell + \eta_{LS} \quad (4.15)$$

so the distribution is

$$dN = \gamma \frac{\cosh^2(\ell + \eta_{LS} - \mathcal{X})}{\cosh^4 \mathcal{X}} d\mathcal{X} d\ell d^2\Omega_2 \quad (4.16)$$

$$0 < \ell + \eta_{LS} \quad (4.17)$$

where the lower equation arises from demanding that the collision does not disrupt structure formation at $\rho = 0$.

We can integrate out \mathcal{X} as before to get

$$dN = \frac{2\gamma}{3} [1 + 2 \cosh(2(\ell + \eta_{LS}))] d\ell d^2\Omega_2 \quad (4.18)$$

This gives the distribution of comoving distances to collision lightcones at last scattering. If we were interested in the distribution at some other time η_1 , we could just replace $\eta_{LS} \rightarrow \eta_1$ in this formula.

4.3 Effects on the Last Scattering Surface

A key measure of the observability of a given collision is the ratio ρ_{LS}/ℓ , where ρ_{LS} is the comoving distance to the last scattering surface and ℓ is the comoving distance to the collision lightcone. Recall that ℓ is negative for collision lightcones that have crossed the origin at last scattering and positive for collision lightcones that have not yet crossed the origin.

Bubbles with $\ell > \rho_{LS}$ are spacelike separated from the entire last scattering surface and have no effect. Bubbles with $-\rho_{LS} < \ell < \rho_{LS}$ affect only part of the last scattering surface and have the most striking signals. Bubbles with $\ell < -\rho_{LS}$ influence the entire last scattering surface. They may lead to interesting effects, especially at long wavelengths. However, it is clear that as the distance to the lightcone gets much larger than the distance to the last scattering surface, $\ell/\rho_{LS} \rightarrow -\infty$, the anisotropy induced by the collision must vanish.

The comoving distance to the last scattering surface is related to the curvature,

$$\rho_{LS} \approx \zeta_0 \sqrt{\Omega_k(t_0)}, \quad (4.19)$$

where $\Omega_k(t_0)$ is the curvature contribution to Ω_{tot} today and $\zeta_0 \sim 3$ is a cosmological-parameter dependent factor (see Appendix D). Observational bounds on curvature give $\rho_{LS} \ll 1$.

As mentioned above, perhaps the most interesting bubbles are those whose future lightcones intersect part of the reheating surface. The number of such bubbles can be obtained by integrating the distribution (4.18) over the range $-\rho_{LS} < \ell < \rho_{LS}$. The total number of such bubbles is

$$N_{LS} = \frac{8\pi\gamma}{3} [2\rho_{LS} + \sinh(2\eta_{LS} + 2\rho_{LS}) - \sinh(2\eta_{LS} - 2\rho_{LS})] \quad (4.20)$$

Using $\rho_{LS} \ll 1$ and $\eta_{LS} \gg 1$ this simplifies to

$$N_{LS} \approx \frac{16\pi\gamma}{3} \rho_{LS} e^{2\eta_{LS}} \quad (4.21)$$

Now using $\rho_{LS} \simeq \zeta_0 \sqrt{\Omega_k(t_0)}$ and $\eta_{LS} = \log \frac{H_f}{H_i}$, we get

$$N_{LS} \approx \frac{16\pi\gamma}{3} \zeta_0 \left(\frac{H_f}{H_i} \right)^2 \sqrt{\Omega_k(t_0)} \quad (4.22)$$

Comparing this to the total number of bubbles, we have

$$\frac{N_{LS}}{N} \approx 4\zeta_0 \sqrt{\Omega_k(t_0)} \sim 12 \sqrt{\Omega_k(t_0)} \quad (4.23)$$

valid for small $\sqrt{\Omega_k(t_0)}$.

For bubbles that intersect the last scattering surface, we can change variables from the distance ℓ to the angular size ψ_{LS} on the CMB sky. In other words, ψ_{LS} is the angular radius of the part of the last scattering surface affected by the collision. Because the last scattering surface is small compared to the radius of curvature, we can approximate the spatial geometry inside the last scattering surface as flat. Also, the collision lightcone has grown large by last scattering, so it is nearly a straight line as it crosses the region inside the last scattering surface. Therefore we can use trigonometry to obtain

$$\frac{\ell}{\rho_{LS}} = \cos \psi_{LS} \quad (4.24)$$

Using the same approximations as above, the distribution in angles is

$$dN \simeq \frac{2\zeta_0\gamma}{3} \left(\frac{H_f}{H_i} \right)^2 \sqrt{\Omega_k(t_0)} d(\cos \psi_{LS}) d^2\Omega_2 . \quad (4.25)$$

The distribution of angular sizes is rather featureless,

$$dN \propto d(\cos \psi_{LS}) . \quad (4.26)$$

5 Discussion

Our primary goal in this paper was to re-consider the probability of observing a cosmic bubble collision in a model like the string theory landscape. We have found that incorporating the effects of a realistic cosmology inside the observation bubble has a dramatic effect on the result, due to the appearance of factors of the dimensionless ratio of the energy scale of the false vacuum to the energy scale of inflation inside the bubble. When this ratio is large (as it must be absent significant fine-tuning) the number of bubble collisions in the past lightcone of an observer in a universe like ours is enhanced, $N \sim \gamma(H_f/H_i)^2$. Physically this

ratio arises for a simple reason: if the observation bubble inflates with Hubble constant H_i , late-time observers like us can see a region of the domain wall with surface area H_i^{-2} , which is large in false vacuum Hubble units. As a result, we can see many Hubble volumes of the false vacuum in which collision bubbles may have nucleated.

In addition to the total number we computed the collision distribution as a function of proper distance between nucleation points in the false vacuum, angular location on the observer's sky, proper time when the collision first enters the observers past lightcone, and angular size on the CMB sky (and on the wall of the observation bubble in Appendix B). The results are striking in several ways. The distribution, when projected onto the observation bubble wall at late times, is globally conformally invariant (*i.e.* invariant under the Lorentz transformations of the nucleation point) in the limit of small angular size. The anisotropy in the distribution, which is present for all but a special observer inside, turns out to be extremely small (because nearly all of the collisions visible to such an observer have very small size on the bubble wall, and the distribution in that limit is rotationally invariant). In particular, as we will see in Appendix C the anisotropic terms in the distribution are suppressed by a factor of $(H_i/H_f)^6$.

The distribution on the last scattering surface is of particular relevance for the potential observability of these events. Collisions with lightcones that bisect the part of the last scattering surface we can observe can create hot or cold disks on the CMB temperature map, and if these disks are of reasonable size and contrast they could be detectable [13]. We find that the number of such disks is $N_{LS} \sim \sqrt{\Omega_k} N \sim \gamma (H_f/H_i)^2 \sqrt{\Omega_k}$. Hence N_{LS} scales as $\sqrt{\Omega_k} = 1/\dot{a} \sim e^{-(N-N^*)}$, where N^* is the number of e-folds of inflation needed to give the universe a radius curvature of order .1 in Hubble units (as required by current observational bounds).

As expected, long inflation inflates away the effects of bubble collisions by inflating away their number density—but since the experimental constraint on curvature is not very strong, the total number can still be quite large with no fine-tuning. However even if $N_{LS} > 1$, one must also consider the effects of inflation on the magnitude of the signal from each collision. The analysis of [13] showed that a single collision with $N - N^* \sim 5$ can have an easily observable effect without fine-tuning the parameters of the collision bubble itself or our boost towards it (which is determined by \mathcal{X} in our notation). If N_{LS} is large or if some of the collisions are with bubble types that have particularly dramatic effects on the early universe, $N - N^*$ could be considerably larger than this and still produce observable effects on the CMB temperature map.

The results of this analysis are interesting for a number of reasons. For one, an observation of the effects of a collision of this type would be, if not a direct confirmation of the string theory landscape, at least very dramatic evidence in its favor. The observational signatures of these collisions has been studied in detail in the context of a collision between two bubbles in a number of recent papers [12, 6, 13, 7], and if they are absent in the data this could constitute an interesting constraint on string models.

Our findings open a large array of directions for future research. One important issue is to make more explicit the connection between the thin-wall Coleman de-Luccia bubbles

considered here and the instanton transitions in the string theory landscape itself. Another is to further study the effects of the collisions on inflation and the CMB sky, and to investigate additional observational opportunities like the effects on large scale structure or CMB polarization. A particularly interesting possibility along those lines is cosmic 21 cm data, which has tremendous potential as a probe of high-scale physics in the early universe [16, 17, 18]. It would be very useful to run a numerical simulation to verify the validity of our assumptions about the domain wall dynamics and their effects on the reheating surface. There is an intriguing connection to conformal field theory, which will be explored in [19]. Finally, there remains the larger issue of the probability measure in the full string theory landscape.

Appendices: In Appendix A, we address the issue of bubbles nucleating inside bubbles with a rate different than that of the parent false vacuum. We find that even in the extreme case that all bubbles are absolutely stable (so that no nucleations occur inside them), our distribution is unchanged up to factors of order $\gamma \ln(H_f/H_i)$, which is generically small.

In Appendix B we compute the distribution of collisions on the asymptotic boundary of the observation bubble using a slightly different technique than that in the bulk of the paper. The results are consistent up to the expected accuracy, and we make the connection to the results in [4] more explicit.

In Appendix C we quantify in detail the level of anisotropy in the collision distribution.

In Appendix D we derive an expression for the conformal time including the effects of early-time radiation domination and late-time dark energy domination.

Acknowledgements

We would like to thank Puneet Batra, Andrei Gruzinov, Lam Hui, Andrei Linde, Massimo Porrati, Steve Shenker, Lenny Susskind, and Alex Vilenkin for useful discussions. BF would like to thank Raphael Bousso and I-Sheng Yang for extensive discussions and collaboration on topics very closely related to the work presented here. The work of MK is supported by NSF CAREER grant PHY-0645435. The work of KS is supported in part by a Natural Sciences and Engineering Research Council of Canada Discovery Grant. We thank the Aspen Center for Physics, where this work was initiated, for its hospitality.

A Proper treatment of overlapping bubbles

The analyses in the paper did not take into account the effects of the interactions of bubble nucleations with each other. After a collision bubble has nucleated, its future lightcone is no longer available for the same type of nucleation event. The vacuum inside the collision bubble may be completely stable; in any case it will certainly have a different set of decay rates than that of the parent false vacuum. As a simple test to see how significant this effect can be for our analysis we will assume the bubbles are absolutely stable, and therefore eliminate all

bubbles from our distribution that would have nucleated inside the future lightcone of other bubbles.

Given two points A and B in de Sitter space, we need a formula for when A and B are spacelike separated. In terms of the embedding coordinates, the condition is

$$\eta_{\mu\nu}X_A^\mu X_B^\nu = X_A X_B + R_A R_B \cos(\delta\theta) - T_A T_B < 1 \quad (\text{A.1})$$

where $\delta\theta$ is the angular separation between the centers of the two bubbles. Changing to our coordinates, the condition is

$$\cosh(\tau_A - \tau_B) < \cosh(\mathcal{X}_A - \mathcal{X}_B) + \cosh \tau_A \cosh \tau_B (1 - \cos(\delta\theta)) \quad (\text{A.2})$$

To take this restriction into account, one could distribute bubbles according to (2.9) and then eliminate any bubble that is in the future lightcone of another bubble. However, we will show that the expected number of bubbles which must be eliminated is generically much less than one, so that this correction can be neglected.

To show this, we consider the S_2 defined by the intersection of the observer's backward lightcone with the domain wall of the observation bubble. In coordinates, this S_2 is defined by $\eta = -\infty$, $\rho = \infty$, $\eta + \rho = \eta_0$. Since this S_2 is on the lightcone of the observation bubble, it can also be defined in the coordinates that cover the exterior of the bubble as the surface $\mathcal{X} = -\infty$, $\tau = \infty$, $\mathcal{X} + \tau = \eta_0$.

A given collision bubble affects a solid angle Ω on this S_2 . We can use the formula (A.2) to find that the solid angle inside the future lightcone of a bubble with coordinates (\mathcal{X}, η_v) is

$$\Omega = 2\pi \frac{e^{\mathcal{X}}(e^{-\eta_v} - e^{-\eta_0})}{\cosh(\eta_v - \mathcal{X})} \quad (\text{A.3})$$

while the angular location of the bubble is randomly distributed.

A sufficient (but not necessary) condition for two nucleation events to be spacelike separated is that the solid angle on the observation bubble's wall affected by one is not completely contained in the solid angle affected by the other. Therefore, if the expected total solid angle affected by all of the bubbles is much less than 4π , then it is unlikely that any bubble is in the future lightcone of another. The expected total solid angle is

$$\left\langle \frac{\Omega}{4\pi} \right\rangle = \gamma \int_0^{\eta_0} d\eta_v \int_{-\infty}^{\infty} d\mathcal{X} \int d^2\Omega \frac{\cosh^2(\eta_v - \mathcal{X})}{\cosh^4 \mathcal{X}} \frac{e^{\mathcal{X}}(e^{-\eta_v} - e^{-\eta_0})}{2 \cosh(\eta_v - \mathcal{X})} = \gamma \left(\frac{\eta_0}{3} + \mathcal{O}(e^{-\eta_0}) \right). \quad (\text{A.4})$$

As we have seen, for a realistic cosmology $\eta_0 \sim \ln \frac{H_f}{H_i}$. Since γ is exponentially small, $\gamma\eta_0$ will generally be much less than 1.

B Collision distribution on the asymptotic sphere

In this appendix we will compute the bubble collision distribution as a function of the angular radius on the asymptotic boundary sphere—which is the boundary of any open spatial slice

inside the observation bubble, or equivalently the observation bubble’s lightcone after infinite time—taken up by collisions. This in general is not the same as the observed angular size of a bubble as seen by a finite time observer. In fact, not all the bubbles that chop off a portion of the boundary are going to be visible to any given observer even after infinite time unless $\Lambda_{\text{in}} = 0$. Hence, the distribution we are going to compute here is not a directly observable quantity. Nevertheless we find it a useful concept, as it characterizes the statistics of collision events unambiguously, and independently of the observer and of the Hubble rate inside our bubble. Indeed, precisely because we are not keeping track of the propagation of the collision signal inside our bubble, the distribution we get cannot depend on the geometry of our bubble, but only on the geometry of its wall—which we approximate as the future light-cone of the nucleation event—and of the outside. As a result, this distribution will be applicable to any cosmology inside. (For the distribution actually seen by a realistic observer, see the analysis of Section 4.)

For simplicity we set $H_f = 1$. The dependence on H_f can be recovered at any stage of our computation just by dimensional analysis. In flat FRW coordinates the metric outside our bubble is

$$ds^2 = dt^2 - e^{2t}(dr^2 + r^2 d\Omega^2) . \quad (\text{B.1})$$

It is actually more convenient to use the (a, F) coordinatization defined by [4],

$$a = e^t , \quad F = r - e^{-t} , \quad (\text{B.2})$$

for which the metric reads

$$ds^2 = 2 da dF - a^2 dF^2 - (1 + aF)^2 d\Omega^2 . \quad (\text{B.3})$$

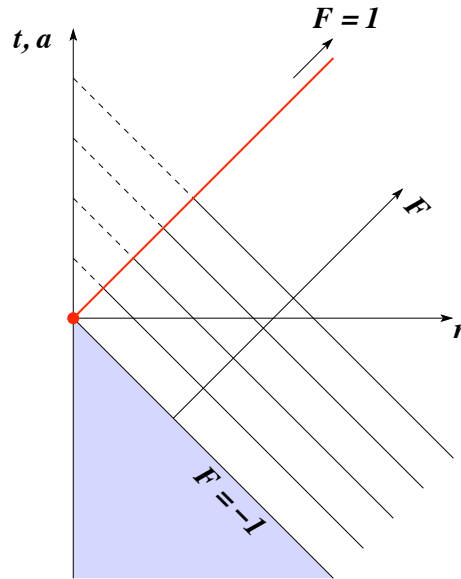


Figure 4: The (a, F) coordinate system described in the text. Our bubble nucleates at the origin $(t = 0, r = 0)$.

a is just the scale factor, while the constant- F hypersurfaces are past directed light-cones, with tip at $r = 0$ (see fig. 4). This chart can in fact cover all of deSitter space, if we let a and F take any real values, with the constraint $aF \geq -1$ ($r \geq 0$). However we will be interested in a smaller range of a and F . First, the surface where initial conditions are given (which we take following [4]) corresponds to $a = 0$. Then, our bubble's nucleation point, $t = 0, r = 0$, corresponds to $a = 1, F = -1$. Therefore, its past light-cone is the surface $F = -1$, with $0 < a < 1$. On the other hand, our bubble's wall—the future-directed light-cone with tip at $(t = 0, r = 0)$ —is the surface $a = 2/(1 - F)$, with $-1 < F < 1$. The region outside both these light-cones, where other nucleation events can take place *and* eventually lead to collisions with our bubble is

$$-1 < F < 1, \quad 0 < a < \frac{2}{1 - F}. \quad (\text{B.4})$$

Notice in particular that $F < 1$ is necessary for the bubble nucleated at (a, F) to eventually collide with ours.

Consider then a bubble nucleated at (a, F) . Its angular size ψ on the boundary sphere is given by [4]

$$\mu \equiv \cos \psi = \frac{1}{2} \frac{a + 2F + aF^2}{1 + aF}. \quad (\text{B.5})$$

Since in the end we are interested in the distribution as a function of μ , we can change variables and trade the nucleation a for μ ,

$$a = \frac{\mu - F}{1 + F^2 - 2F\mu}. \quad (\text{B.6})$$

This way each collision event will be labeled by its angular size μ and by F , which is ‘conserved’ between nucleation and collision—because the bubble wall follows a null trajectory with $F = \text{const}$. The allowed ranges for these variables are

$$-1 < \mu < 1, \quad -1 < F < \mu. \quad (\text{B.7})$$

Indeed eq. (B.5) is an increasing function of a for fixed F . This means that the maximum and minimum of μ are attained at the extrema of a , for a given F . This yields the ranges above. The infinitesimal four-volume element corresponding to the infinitesimal intervals $d\mu, dF$ is

$$dV_4 = 4\pi(1 + aF)^2 da dF = \frac{8\pi(1 - F^2)^3}{(1 + F^2 - 2F\mu)^4} d\mu dF, \quad (\text{B.8})$$

where we used eq. (B.6) for the change of variable $a \rightarrow \mu$, and the 4π comes from the solid angle integral. Then, the four-volume where a bubble of size between μ and $\mu + d\mu$ can nucleate is just the integral of this along F , from -1 to μ (see eq. (B.7)),

$$\frac{dV_4}{d\mu} = \int_{-1}^{\mu} dF \frac{dV_4}{d\mu dF} = \frac{4\pi}{3} \frac{(2 - \mu)}{(1 - \mu)^2}. \quad (\text{B.9})$$

A bubble of size μ takes out a solid angle $2\pi(1 - \mu)$ on the boundary sphere. The solid angle $\Omega_f(\mu)$ that is free of bubbles with angular sizes from $\mu = -1$ to μ obeys the equation

$$\frac{d\Omega_f(\mu)}{d\mu} = -2\pi(1 - \mu) \cdot \gamma \cdot \frac{\Omega_f(\mu)}{4\pi} \frac{dV_4}{d\mu}, \quad (\text{B.10})$$

where γ is the nucleation rate, and we included the factor $\Omega_f/4\pi$ to account for the fact that at any given μ only such a fraction of the solid angle is still available for new nucleations and collisions (in other words, we are counting regions in which disks overlap only once, no matter how many such overlaps there may be). The solution with boundary condition $\Omega_f(-1) = 4\pi$ is

$$\Omega_f(\mu) = 4\pi \left(\frac{1 - \mu}{2} \right)^{\frac{2}{3}\pi\gamma} e^{-\frac{2}{3}\pi\gamma(1+\mu)} \quad (\text{B.11})$$

or, in differential form,

$$\frac{d\Omega_f(\mu)}{d\mu} = -\frac{8\pi^2\gamma}{3} \frac{2 - \mu}{1 - \mu} \left(\frac{1 - \mu}{2} \right)^{\frac{2}{3}\pi\gamma} e^{-\frac{2}{3}\pi\gamma(1+\mu)} \quad (\text{B.12})$$

As a check notice that if we consider all bubble sizes, from $\mu = -1$ to $\mu = 1$, all the solid angle but a set of measure zero is eaten up by collisions,

$$\Omega_f(1) = 0, \quad (\text{B.13})$$

as expected. Another quantity of interest is the expected number of bubbles with angular size between μ and $\mu + d\mu$,

$$\frac{dN(\mu)}{d\mu} = -\frac{\gamma}{2\pi(1 - \mu)} \frac{d\Omega_f(\mu)}{d\mu}. \quad (\text{B.14})$$

Integrating this we get total number of bubbles down to angular size μ :

$$N(\mu) = \frac{4\pi\gamma}{3} \left(-\frac{3}{4e^{2\pi\gamma}} \right)^{\frac{2\pi\gamma}{3}} \left[\gamma\left(\frac{2\pi\gamma}{3}, -\frac{2\pi\gamma}{3}(1 - \mu), -\frac{4\pi\gamma}{3}\right) - \frac{2\pi\gamma}{3} \gamma\left(-1 + \frac{2\pi\gamma}{3}, -\frac{2\pi\gamma}{3}(1 - \mu), -\frac{4\pi\gamma}{3}\right) \right], \quad (\text{B.15})$$

where $\gamma(a, z_1, z_2)$ is the generalized incomplete gamma function, $\gamma(a, z_1, z_2) \equiv \int_{z_1}^{z_2} t^{a-1} e^{-t} dt$. Perhaps more interesting is the asymptotic behavior of $n(\mu)$ at small angular sizes $\psi \ll 1$. Expanding $\mu = \cos \psi$ we get

$$N(\psi) = \frac{8\pi\gamma}{\left(2 - \frac{2\pi\gamma}{3}\right)(2e)^{\frac{4\pi\gamma}{3}}} \cdot \frac{1}{\psi^{2 - \frac{4\pi\gamma}{3}}} + \mathcal{O}(1), \quad (\text{B.16})$$

which gives us the fractal dimension of our ensemble, $d = 2 - \frac{4\pi\gamma}{3}$, in agreement with GGV's result [4].

Although we did not keep track of the bubble positions on the boundary sphere, the distribution we have computed is obviously isotropic, because we have computed it in a frame where the initial-condition surface ($a = 0$) is invariant under rotations. This is the distribution that could in principle be seen by the central observer after infinite time, if she lives in a bubble of Minkowski vacuum and can see all the way to her bubble’s domain wall. To compute the boundary distribution relevant for a different observer, we have to “boost” eq. (B.11).

B.1 Trasformation properties under boosts

We are thus led to consider how a deSitter boost acts on the boundary sphere. Recall that deSitter boosts about our bubble’s nucleation point (henceforth “the origin”) act as spatial translations on any given hyperbolic FRW slice inside the bubble. That is why different comoving FRW observers are mapped into each other by boosts about the origin. However since we are interested just in the boundary sphere, we can use the fact that the isometries of three-dimensional hyperbolic space acts as the two-dimensional conformal group on the boundary. In particular, a translation (= deSitter boost) along z acts as a dilation about the south pole and a contraction about the north pole. More precisely, consider the metric on the sphere

$$d\Omega_2^2 = d\theta^2 + \sin^2 \theta d\varphi^2 ; \tag{B.17}$$

it is a conformally flat metric, as made evident by the change of variable

$$\rho = \frac{1 + \cos \theta}{\sin \theta} \quad \leftrightarrow \quad \sin \theta = \frac{2\rho}{1 + \rho^2} , \tag{B.18}$$

which is the standard stereographic projection, mapping the sphere to the plane. The North Pole (NP) $\theta = 0$ gets projected to infinity, whereas the South Pole (SP) $\theta = \pi$ gets mapped to the origin $\rho = 0$. Upon the stereographic projection the metric becomes

$$d\Omega_2^2 = \frac{4}{(1 + \rho^2)^2} (d\rho^2 + \rho^2 d\varphi^2) . \tag{B.19}$$

Then, dilations about the origin, $\rho \rightarrow \lambda\rho$, leave the metric explicitly conformally flat. These are the trasformations that correspond to translations along z in the three-dimensional hyperbolic interior of the sphere. In terms of θ and φ they act as

$$\sin \theta \rightarrow \sin \theta' = \sin \theta \frac{2\lambda}{(\lambda^2 + 1) + (\lambda^2 - 1) \cos \theta} , \quad \varphi \rightarrow \varphi' = \varphi . \tag{B.20}$$

The action of this transformation is schematically depicted in fig. 5.

Bubble collisions chop off circles on the boundary sphere. Interestingly enough, circles get mapped into circles by our conformal transformation eq. (B.20). To see this, recall that the stereographic projection (B.18) maps circles on the sphere to circles on the plane. Combining this with a dilation on the plane $\rho \rightarrow \lambda\rho$, which clearly maps circles into circles,

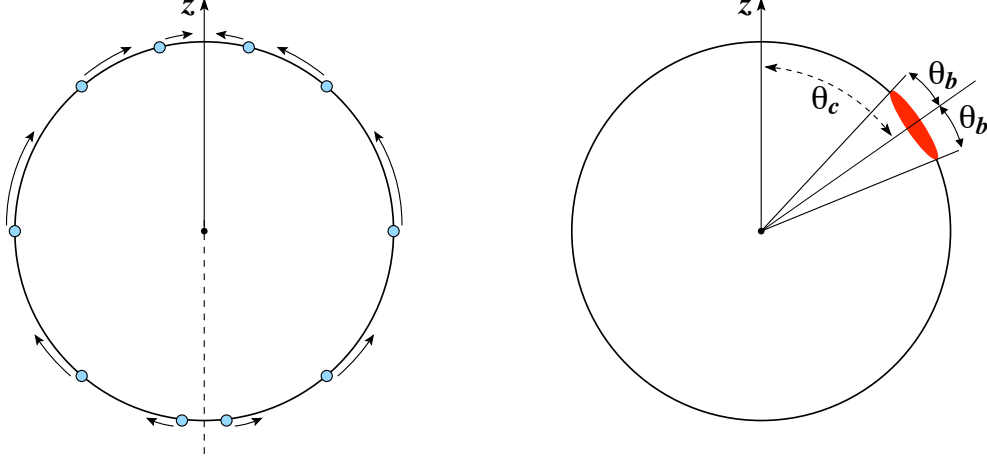


Figure 5: *Left:* A boost along z acts on the boundary sphere as a dilation about the south pole and a contraction about the north pole. *Right:* A circle on the boundary sphere is parameterized by its center's coordinates (θ, φ) and its angular radius ψ .

and with an inverse stereographic projection, we get that eq. (B.20) maps circles to circles. So, given a circle we just have to understand what happens to its center and its radius upon the transformation. Notice that the new center's θ will not be simply the transformed θ of the old center according to eq. (B.20). Rather, given a bubble with center at θ and angular radius ψ (see fig. 5), to find the new center's position we have to transform the two extrema of the bubble along theta, $(\theta \pm \psi)$, and take their half-sum,

$$\theta' \equiv \frac{(\theta + \psi)' + (\theta - \psi)'}{2}. \quad (\text{B.21})$$

Likewise, the new angular radius is given by

$$\psi' \equiv \frac{(\theta + \psi)' - (\theta - \psi)'}{2}. \quad (\text{B.22})$$

To simplify the algebra, we can consider two limiting cases: that of an infinitesimal transformation, $\lambda = 1 + \epsilon$, and that of an infinite one, $\lambda \gg 1$. In the former case we have an infinitesimal, θ -dependent shift on θ ,

$$\delta\theta \equiv \theta' - \theta \simeq -\epsilon \sin \theta. \quad (\text{B.23})$$

For a bubble centered at θ with angular radius ψ we get

$$\theta \simeq \theta - \epsilon \sin \theta \cos \psi, \quad \psi' \simeq \psi - \epsilon \sin \psi \cos \theta. \quad (\text{B.24})$$

If we restrict to very small bubbles, $\psi \ll 1$, these transformation laws further simplify to

$$\theta \simeq \theta - \epsilon \sin \theta, \quad \psi' \simeq \psi(1 - \epsilon \cos \theta). \quad (\text{B.25})$$

The number of bubbles per solid angle down to angular size ψ is given by eq. (B.16)

$$dN \propto \frac{\gamma}{\psi^{2-\frac{4\pi\gamma}{3}}} d(\cos \theta) , \quad (\text{B.26})$$

where the $d(\cos \theta)$ comes from the isotropy of our distribution. The number dn is invariant under our boost, whereas θ and ψ transform as in eq. (B.25). Therefore the boosted distribution reads

$$dN \propto \frac{\gamma}{\psi^{2-\frac{4\pi\gamma}{3}}} (1 + \epsilon \frac{4\pi\gamma}{3} \cos \theta') d(\cos \theta') . \quad (\text{B.27})$$

The boost introduces a dipolar anisotropy in the bubble-collision distribution.

More interesting for us is the opposite limit, that of infinite boost $\lambda \rightarrow \infty$. To figure out its action, it is best to work directly on the stereographic plane. Given a circle on the sphere with center at θ and angular size ψ , this corresponds to a circle on the plane with center at ρ_c and radius ρ_b ,

$$\rho_c = \frac{1}{2}(\rho_+ + \rho_-) , \quad \rho_b = \frac{1}{2}(\rho_+ - \rho_-) , \quad (\text{B.28})$$

where ρ_{\pm} are the projections of $\theta_{\pm} \equiv \theta \pm \psi$, according to eq. (B.18). After some some straightforward algebra we get

$$\rho_c = \frac{\sqrt{1-x^2}}{\mu-x} , \quad \rho_b = \frac{\sqrt{1-\mu^2}}{\mu-x} , \quad (\text{B.29})$$

where we have defined

$$x \equiv \cos \theta , \quad \mu = \cos \psi . \quad (\text{B.30})$$

The inverse mapping is

$$x = \frac{\rho_c^2 - \rho_b^2 - 1}{\sqrt{(\rho_c^2 + \rho_b^2 + 1)^2 - 4\rho_c^2\rho_b^2}} , \quad \mu = \frac{\rho_c^2 - \rho_b^2 + 1}{\sqrt{(\rho_c^2 + \rho_b^2 + 1)^2 - 4\rho_c^2\rho_b^2}} . \quad (\text{B.31})$$

Now, the number of collisions per unit x and μ is (see eqs. (B.14, B.12), and recall that before boosting the distribution is isotropic)

$$dN \sim \frac{1}{1-\mu} d\Omega_f \sim \gamma \frac{2-\mu}{(1-\mu)^2} \left(\frac{1-\mu}{2} \right)^{\frac{2}{3}\pi\gamma} e^{-\frac{2}{3}\pi\gamma(1+\mu)} dx d\mu , \quad (\text{B.32})$$

which in terms of ρ_c and ρ_b reads

$$dN \sim \gamma \left[(2-\mu)(1+\mu)^2 \left(\frac{1-\mu}{2} \right)^{\frac{2}{3}\pi\gamma} e^{-\frac{2}{3}\pi\gamma(1+\mu)} \right] \times \frac{\rho_c}{\rho_b^3} d\rho_b d\rho_c . \quad (\text{B.33})$$

The piece outside the brackets is manifestly invariant under dilations $\rho \rightarrow \lambda\rho$, which are precisely the transformations we are interested in. We just have to figure out what happens

to the terms in brackets. Performing a very large boost corresponds to using a new radial coordinate

$$\rho' = \lambda \rho, \quad \lambda \gg 1. \quad (\text{B.34})$$

Finite values of ρ' correspond to tiny values of ρ , which on the sphere correspond to very small displacements from the SP, $x \simeq -1$ and $\mu \simeq 1$. More precisely, from eq. (B.31) we have

$$\mu \simeq 1 - \frac{2}{\lambda^2} \rho_b'^2. \quad (\text{B.35})$$

Plugging this into our distribution and dropping the primes we get

$$dN \sim \frac{\gamma}{\lambda^{\frac{4}{3}\pi\gamma}} \frac{\rho_c}{\rho_b^{3-\frac{4}{3}\pi\gamma}} d\rho_b d\rho_c \quad (\text{B.36})$$

which projected back onto the sphere via eq. (B.29) reads

$$dN \sim \frac{\gamma}{\lambda^{\frac{4}{3}\pi\gamma}} \frac{d\psi}{(\sin \psi)^{3-\frac{4}{3}\pi\gamma}} \frac{d \cos \theta}{(\cos \psi - \cos \theta)^{\frac{4}{3}\pi\gamma}}. \quad (\text{B.37})$$

To see the relation to the distribution derived in the bulk of the paper (Eq. (2.9)), we need to integrate the latter over \mathcal{X} . If we do not impose any restriction on the observer from domain walls, the limits of integration are from $(-\infty, \infty)$, giving (c.f. Eq. (2.9))

$$dN = \frac{8\pi}{3} \gamma \cosh^2 \tau d\tau d \cos \theta. \quad (\text{B.38})$$

where we have used $\eta_v - \mathcal{X} = \tau$. The relation between the coordinate τ and the asymptotic angular radius ψ is simply $\tanh \tau = \cos \psi$; with a little algebra this becomes

$$dN = \frac{8\pi\gamma}{3} \frac{d\psi}{\sin^3 \psi} d \cos \theta. \quad (\text{B.39})$$

So far we have placed no restrictions on the direction of the boost. However if we require that the boost avoid bubble domain walls, the distribution Eq. (B.37) will be modified by a factor of $\Theta(\theta - \psi)$, which enforces that no disks cover the point $\theta = 0$ the boost was taken towards. This condition coincides precisely to the one imposed by the initial condition surface at infinite boost discussed in the text below Eq. (3.8), which is $\cos \psi + \tanh \tau > 0$, or in these coordinates $\theta > \psi$.

Expanding Eq. (B.37) in powers of γ gives

$$dN \sim \gamma \frac{d\psi}{\sin^3 \psi} d \cos \theta (1 + \mathcal{O}(\gamma \ln \delta)), \quad (\text{B.40})$$

in agreement with Eq. (B.39) up to factors of order $\gamma \ln \delta$. Here δ is a UV cutoff applied both to the minimum size $\psi_{\min} \sim \delta$ of the disks and to the boost parameter $\lambda_{\max} \sim 1/\delta$.

The cutoff on boosts is necessary because Eq. (B.37) is an average derived under the assumption that no bubbles nucleate inside other bubbles. Boosting the resulting distribution

infinitely leads to a singular result, since the average was taken before the boost and all but a set of measure zero of such boosts are in directions already “eaten” by a bubble domain wall.

A cutoff on ψ corresponds to a cutoff on the observer’s conformal time η_0 through $\mathcal{X} + \tau = \eta_0$. After integrating over \mathcal{X} this translates into $-\ln \psi_{\min} \sim \eta_0$, or $\psi_{\min} \sim H_i/H_f$. As a quick check, according to Eq. (B.37) the fraction of the asymptotic sky covered by disks is then $\gamma \int \psi^2 d\psi / \sin^3 \psi \sim -\gamma \ln \psi_{\min} \sim \gamma \eta_0$, in agreement with Eq. (A.4). Hence, the expansion in γ shows that the distributions (B.37) and (B.39) agree as expected up to corrections of order $\gamma \eta_0 \approx \gamma \ln(H_f/H_i)$.

C Legendre moments of the collision distribution

In this appendix we derive the Legendre moments of the bubble collision direction distribution, and compare this with the distribution found in Ref. [4]. We focus on the effects of inflation with $H_i \neq H_f$ inside the bubble, but these results can be straightforwardly generalized to include arbitrary cosmological evolution inside the bubble. Using the restriction of Eq. (3.6) we can show that for an internal de Sitter space with $H_i \neq H_f$ the four-volume available for the nucleation of bubbles in the $\xi \rightarrow \infty$, infinite boost, limit is

$$\frac{dV_4}{dt d\Omega} = \frac{1}{3\mathcal{H}_i^3 [\mathcal{H}_i^2 \cosh^2(\frac{\mathcal{H}_i t}{2}) - \sinh^2(\frac{\mathcal{H}_i t}{2})]} \times \left[\left(\frac{\mathcal{H}_i^2 \sinh(\mathcal{H}_i t)}{\mathcal{H}_i^2 (1 - \cos \theta) \cosh^2(\frac{\mathcal{H}_i t}{2}) + (1 + \cos \theta) \sinh^2(\frac{\mathcal{H}_i t}{2})} \right)^3 - \tanh^3\left(\frac{\mathcal{H}_i t}{2}\right) \right] \quad (\text{C.1})$$

where we have adopted the notation $\mathcal{H}_i = H_i/H_f$ for the dimensionless ratio of Hubble rates. In the limit $\mathcal{H}_i \rightarrow 1$ this reduces to Eq. (45) of Ref. [4].

We define

$$\mu = \cos \theta, \quad (\text{C.2})$$

and write

$$\frac{dV_4}{dt d\Omega} = \frac{\alpha}{(\beta - \mu)^3} - \lambda \quad (\text{C.3})$$

where

$$\alpha = \frac{\mathcal{H}_i^6 \sinh^3(\mathcal{H}_i t)}{3\mathcal{H}_i^3 [\mathcal{H}_i^2 \cosh^2(\frac{\mathcal{H}_i t}{2}) - \sinh^2(\frac{\mathcal{H}_i t}{2})]} \quad (\text{C.4})$$

$$\beta = \frac{\mathcal{H}_i^2 \cosh^2(\frac{\mathcal{H}_i t}{2}) + \sinh^2(\frac{\mathcal{H}_i t}{2})}{\mathcal{H}_i^2 \cosh^2(\frac{\mathcal{H}_i t}{2}) - \sinh^2(\frac{\mathcal{H}_i t}{2})} \quad (\text{C.5})$$

and

$$\lambda = \frac{\tanh^3(\frac{\mathcal{H}_i t}{2})}{3\mathcal{H}_i^3 [\mathcal{H}_i^2 \cosh^2(\frac{\mathcal{H}_i t}{2}) - \sinh^2(\frac{\mathcal{H}_i t}{2})]^4} \quad (\text{C.6})$$

We expand Eq. C.3 in orthonormal Legendre polynomials that satisfy

$$\int_{-1}^1 d\mu P_n(\mu)P_m(\mu) = \delta_{mn} \quad (\text{C.7})$$

as

$$\frac{dV_4}{dt d\Omega} = \sum_{n=0}^{\infty} v_n P_n(\mu). \quad (\text{C.8})$$

The generating function for the $P_n(\mu)$ is

$$Z(\mu, u) = \sum_{n=0}^{\infty} \sqrt{\frac{2}{2n+1}} P_n(\mu) u^n = \frac{1}{\sqrt{1-2u\mu+u^2}} \quad (\text{C.9})$$

so that

$$P_n(\mu) = \frac{\sqrt{n+\frac{1}{2}}}{n!} \left. \frac{\partial^n Z}{\partial u^n} \right|_{u=0} \quad (\text{C.10})$$

From $Z(\mu, t)$ we can define a generating function for the Legendre moments v_n as

$$\mathcal{V} = \int_{-1}^1 d\mu Z(\mu, u) \frac{dV_4}{dt d\Omega} = \alpha \int_{-1}^1 d\mu \frac{Z(\mu, u)}{(\beta - \mu)^3} - 2\lambda \quad (\text{C.11})$$

$$= \alpha \left[Z_\beta^2 \left(\frac{2\beta - u(\beta^2 + 1)}{(\beta^2 - 1)^2} \right) + Z_\beta^4 \frac{3u(\beta u - 1)}{\beta^2 - 1} + 3Z_\beta^5 u^2 \operatorname{arcoth}[Z_\beta(\beta - u)] \right] - 2\lambda, \quad (\text{C.12})$$

where $Z_\beta = Z(\beta, u)$, such that

$$v_n = \frac{\sqrt{n+\frac{1}{2}}}{n!} \left. \frac{\partial^n \mathcal{V}}{\partial u^n} \right|_{u=0}. \quad (\text{C.13})$$

The first few moments are

$$v_0 = \frac{\sqrt{2}\alpha\beta}{(\beta^2 - 1)^2} - \lambda \quad (\text{C.14})$$

$$v_1 = \frac{\sqrt{6}\alpha}{(\beta^2 - 1)^2} \quad (\text{C.15})$$

$$v_2 = \frac{\sqrt{5}\alpha(5\beta - 3\beta^3 + 3(\beta^2 - 1)^2 \operatorname{arcoth} \beta)}{\sqrt{2}(\beta^2 - 1)^2} \quad (\text{C.16})$$

in the limit $\mathcal{H}_i t \gg 1$ we have

$$v_0 = \frac{2\sqrt{2}}{3} \left[\frac{2}{\mathcal{H}_i^3} + \frac{1}{\mathcal{H}_i} \right] e^{-\mathcal{H}_i t} + O(e^{-2\mathcal{H}_i t}) \quad (\text{C.17})$$

$$v_1 = \frac{2\sqrt{6}}{3} \left[\frac{1}{\mathcal{H}_i} \right] e^{-\mathcal{H}_i t} + O(e^{-2\mathcal{H}_i t}) \quad (\text{C.18})$$

$$v_2 = \frac{2\sqrt{10}}{3} \left[\frac{-1 + 8\mathcal{H}_i^2 + 12\mathcal{H}_i^4 \ln \mathcal{H}_i^2 - 8\mathcal{H}_i^6 + \mathcal{H}_i^8}{\mathcal{H}_i(\mathcal{H}_i^2 - 1)^4} \right] e^{-\mathcal{H}_i t} + O(e^{-2\mathcal{H}_i t}) \quad (\text{C.19})$$

from which we can see the dipole and higher multipoles are suppressed relative to the monopole by a factor of \mathcal{H}_i^2 in the limit that \mathcal{H}_i is a small parameter, and the distribution is nearly isotropic.

To leading order in the \mathcal{H}_i expansion we can write for an arbitrary multiple moment

$$v_n = (-1)^{n+1} \frac{2\sqrt{4n+2}}{3\mathcal{H}_i} \left[1 - \mathcal{H}_i^2(n+2)(n-1) + O(\mathcal{H}_i^4) \right] e^{-\mathcal{H}_i t} + O(e^{-2\mathcal{H}_i t}) \quad (\text{C.20})$$

from which we see that all multipole moments are present, albeit suppressed by a factor of \mathcal{H}_i^2 , at late times when $\mathcal{H}_i \neq 1$ rather than the late-time monopole-plus-dipole distribution found in Ref. [4] for the $\mathcal{H}_i = 1$ case.

The late time distribution takes the exact form

$$\frac{dV_4}{dt d\Omega} = \frac{4}{3\mathcal{H}_i^3(1-\mathcal{H}_i^2)} \left[1 - \frac{8\mathcal{H}_i^6}{[1 + \cos\theta + \mathcal{H}_i^2(1 - \cos\theta)]^3} \right] e^{-\mathcal{H}_i t} + O(e^{-2\mathcal{H}_i t}) \quad (\text{C.21})$$

which in the limit $\mathcal{H}_i \rightarrow 1$ is simply

$$\frac{dV_4}{dt d\Omega} = 2(1 + \cos\theta)e^{-t} + O(e^{-2t}) \quad (\text{C.22})$$

in agreement with Ref. [4].

To leading order in \mathcal{H}_i the late-time distribution is

$$\frac{dV_4}{dt d\Omega} = \frac{4}{3\mathcal{H}_i^3} \left[1 + \mathcal{H}_i^2 + \mathcal{H}_i^4 + \left(1 - \frac{8}{[1 + \cos\theta + \mathcal{H}_i^2(1 - \cos\theta)]^3} \right) \mathcal{H}_i^6 + O(\mathcal{H}_i^8) \right] e^{-\mathcal{H}_i t} + O(e^{-2\mathcal{H}_i t}) \quad (\text{C.23})$$

and so the anisotropic part of the distribution is suppressed by H_i^6 except in the region $\pi - \theta < \epsilon$, where $\epsilon \sim H_i/H_f$. Only a fraction of order H_i^2/H_f^2 of the collisions are centered within this region.

D Computation of the conformal time with a $\Omega_\Lambda \neq \Omega_k \neq \Omega_r \neq 0$

In this appendix we derive an expression for the conformal time taking into account early time radiation domination and late time dark-energy domination (modeled here as a cosmological

constant) of our Universe. In this paper we use a convention where the scale factor has units of length and the curvature $k = -1$ is a dimensionless quantity. We will not set $k = -1$ in this derivation to allow easy comparison to the alternative convention often used where the scale factor is dimensionless and k has units of inverse length squared. For a scale factor $a(t)$, where t is cosmological time, the dimensionless conformal time today since some early time t_i is

$$\Delta\eta = \eta_0 - \eta_e = \sqrt{-k} \int_{t_i}^{t_0} \frac{dt'}{a(t')}, \quad (\text{D.1})$$

which can be expressed in terms of the Hubble rate H as

$$\Delta\eta = \sqrt{-k} \int_{a_i}^{a_0} \frac{da}{a^2 H}. \quad (\text{D.2})$$

We introduce the variables $\tilde{a} = a/a_0$ where a_0 is the scale factor today, and $\tilde{H} = H/H_0$ where H_0 is the Hubble rate today. In terms of these variables the Hubble rate is

$$\tilde{H}(\tilde{a}) = \sqrt{\Omega_r \tilde{a}^{-4} + \Omega_m \tilde{a}^{-3} + \Omega_k \tilde{a}^{-2} + \Omega_\Lambda} \quad (\text{D.3})$$

and so

$$f(\tilde{a}) = \frac{1}{\tilde{a}^2 \tilde{H}(\tilde{a})} = \frac{1}{\sqrt{\Omega_r + \Omega_m \tilde{a} + \Omega_k \tilde{a}^2 + \Omega_\Lambda \tilde{a}^4}}. \quad (\text{D.4})$$

The conformal time is then

$$\Delta\eta = \frac{\sqrt{-k}}{a_0 H_0} \int_{\tilde{a}_i}^1 d\tilde{a} f(\tilde{a}) = \sqrt{\Omega_k} \int_{\tilde{a}_i}^1 d\tilde{a} f(\tilde{a}). \quad (\text{D.5})$$

where we have used the definition of the curvature density $\Omega_k = -k/(a_0^2 H_0^2)$. We write

$$\zeta_0 = \zeta_0(\Omega_r, \Omega_m, \Omega_k, \Omega_\Lambda) = \int_{\tilde{a}_i}^1 d\tilde{a} f(\tilde{a}) \quad (\text{D.6})$$

Typically \tilde{a}_i is the scale factor at reheating and we can safely take $\tilde{a}_i \simeq 0$. We set $a_i \rightarrow 0$ in what follows. To make further progress we split the integral about $\tilde{a}_e = (\Omega_r/\Omega_m)$, the scale factor at matter-radiation equality as

$$\zeta_0 \simeq \int_0^{\tilde{a}_e} d\tilde{a} f(\tilde{a}) + \int_{\tilde{a}_e}^1 d\tilde{a} f(\tilde{a}) \quad (\text{D.7})$$

As it starts deep in the radiation dominated epoch and ends at matter-radiation equality the first part of the integral can be very accurately approximated in the limit $\Omega_\Lambda \rightarrow 0$ and $\Omega_k \rightarrow 0$ as

$$\int_0^{\tilde{a}_e} d\tilde{a} f(\tilde{a}) \simeq (\sqrt{2} - 1) \frac{2\sqrt{\Omega_r}}{\Omega_m} \quad (\text{D.8})$$

The second part of the integral can be solved as a series expansion about $\Omega_k = \Omega_r = 0$. We write

$$\begin{aligned} f(\tilde{a}) &= \sum_{m=0}^{\infty} \sum_{n=0}^{\infty} \frac{1}{m!n!} \frac{\partial^{(m+n)} f}{\partial \Omega_k^m \partial \Omega_r^n} \Bigg|_{\substack{\Omega_k=0 \\ \Omega_r=0}} \Omega_k^m \Omega_r^n \\ &= \sum_{n=0}^{\infty} \frac{1}{n!} \frac{\partial^n f}{\partial \Omega_r^n} \Bigg|_{\substack{\Omega_k=0 \\ \Omega_r=0}} \Omega_r^n + \Omega_k \frac{\partial f}{\partial \Omega_k} \Bigg|_{\substack{\Omega_k=0 \\ \Omega_r=0}} + \dots \end{aligned} \quad (\text{D.9})$$

where in second line we have only included the terms that contribute at leading order. We perform the integral term by term to find

$$\int_{\tilde{a}_e}^1 d\tilde{a} f(\tilde{a}) = \sum_{n=0}^{\infty} \frac{(-1)^{n+1} (2n-1)!!}{2^n (4n+1)n!} \frac{1}{\Omega_\Lambda^{n+1/2}} \Phi_n + \Omega_k \Psi + \dots \quad (\text{D.10})$$

where

$$\Phi_n = {}_2F_1 \left(\frac{2n+1}{2}, \frac{4n+1}{3}, \frac{4n+4}{3}; -\frac{\Omega_m}{\Omega_\Lambda} \right) - \frac{1}{\tilde{a}_e^{4n+1}} {}_2F_1 \left(\frac{2n+1}{2}, \frac{4n+1}{3}, \frac{4n+4}{3}; -\frac{\Omega_m}{\tilde{a}_e^3 \Omega_\Lambda} \right) \quad (\text{D.11})$$

and

$$\Psi = \frac{1}{3\Omega_m^{3/2}} \left[\left(\frac{1}{\tilde{a}_e^3} + \frac{\Omega_\Lambda}{\Omega_m} \right)^{-1/2} - \left(1 + \frac{\Omega_\Lambda}{\Omega_m} \right)^{-1/2} \right]. \quad (\text{D.12})$$

Combining these expressions, expanding to leading order in the cosmological parameters, and substituting $\tilde{a}_e \equiv \Omega_r/\Omega_m$ we find that

$$\zeta_0 \simeq \frac{\Gamma[\frac{1}{6}]\Gamma[\frac{4}{3}]}{\sqrt{\pi}\Omega_m^{1/3}\Omega_\Lambda^{1/6}} - \frac{1}{\sqrt{\Omega_\Lambda}} \left[1 - \frac{\Omega_m}{8\Omega_\Lambda} - \frac{3\Omega_m^2}{56\Omega_\Lambda^2} - \frac{\Omega_k(\Omega_m - 2\Omega_\Lambda)}{6\Omega_m\Omega_\Lambda} \right] - \frac{2\sqrt{\Omega_r}}{\Omega_m} \quad (\text{D.13})$$

to a very good approximation (higher order terms contribute $\lesssim 0.1\%$ near current cosmological parameters). Note that while Eq. (D.10) is valid for any value of Ω_Λ including $\Omega_\Lambda \rightarrow 0$, Eq. (D.13) is a good approximation only in a Universe, like our own, in which the cosmological constant is already dominating the expansion.

Current cosmological observations [20] admit $\Omega_k \sim 0.01$. For instance, recent cosmological constraints are compatible with $\Omega_\Lambda = 0.72 \pm 0.03$ and $\Omega_r = 4.12 \times 10^{-5}/h^2 \simeq (8.3 \pm 0.6) \times 10^{-5}$ near $\Omega_k \simeq 0.005$ or $\Omega_\Lambda \simeq 0.71 \pm 0.01$ and $\Omega_r \simeq (7.9 \pm 0.2) \times 10^{-5}$ near $\Omega_k \simeq 0.01$. These translate to a typical ranges $\zeta_0 \simeq 3.35_{-0.14}^{+0.16}$ near $\Omega_k \simeq 0.005$ and $\zeta_0 \simeq 3.33_{-0.05}^{+0.05}$ near $\Omega_k \simeq 0.01$ — more than 60% larger than the matter-dominated estimate ($\zeta \simeq 2$) discussed in Section 4.1 of this paper.

References

- [1] R. Bousso and J. Polchinski, “Quantization of four-form fluxes and dynamical neutralization of the cosmological constant,” *JHEP* **0006**, 006 (2000) [arXiv:hep-th/0004134].
- [2] L Susskind, “The anthropic landscape of string theory,” arXiv:hep-th/0302219.
- [3] A. H. Guth and E. J. Weinberg, “Could The Universe Have Recovered From A Slow First Order Phase Transition?,” *Nucl. Phys. B* **212**, 321 (1983).
- [4] J. Garriga, A. H. Guth and A. Vilenkin, “Eternal inflation, bubble collisions, and the persistence of memory,” *Phys. Rev. D* **76**, 123512 (2007) [arXiv:hep-th/0612242].
- [5] A. Aguirre, M. C. Johnson and A. Shomer, “Towards observable signatures of other bubble universes,” *Phys. Rev. D* **76**, 063509 (2007) [arXiv:0704.3473 [hep-th]].
- [6] A. Aguirre and M. C. Johnson, “Towards observable signatures of other bubble universes II: Exact solutions for thin-wall bubble collisions,” *Phys. Rev. D* **77**, 123536 (2008) [arXiv:0712.3038 [hep-th]].
- [7] A. Aguirre, M. C. Johnson and M. Tysanner, “Surviving the crash: assessing the aftermath of cosmic bubble collisions,” arXiv:0811.0866 [hep-th].
- [8] R. Bousso, B. Freivogel, and I. Yang, *Unpublished*
- [9] A. Dahlen, “Odds of observing the multiverse,” arXiv:0812.0414 [hep-th].
- [10] S. W. Hawking, I. G. Moss and J. M. Stewart, “Bubble Collisions In The Very Early Universe,” *Phys. Rev. D* **26**, 2681 (1982).
- [11] B. Freivogel, G. T. Horowitz and S. Shenker, “Colliding with a crunching bubble,” *JHEP* **0705**, 090 (2007) [arXiv:hep-th/0703146].
- [12] S. Chang, M. Kleban and T. S. Levi, “When Worlds Collide,” *JCAP* **0804**, 034 (2008) [arXiv:0712.2261 [hep-th]].
- [13] S. Chang, M. Kleban and T. S. Levi, “Watching Worlds Collide: Effects on the CMB from Cosmological Bubble Collisions,” arXiv:0810.5128 [hep-th].
- [14] B. Freivogel, M. Kleban, M. Rodriguez Martinez and L. Susskind, “Observational consequences of a landscape,” *JHEP* **0603**, 039 (2006) [arXiv:hep-th/0505232].
- [15] N. Kaloper, M. Kleban and L. Sorbo, “Observational implications of cosmological event horizons,” *Phys. Lett. B* **600**, 7 (2004) [arXiv:astro-ph/0406099].
- [16] A. Loeb and M. Zaldarriaga, “Measuring the small-scale power spectrum of cosmic density fluctuations through 21-cm tomography prior to the epoch of structure formation,” *Phys. Rev. Lett.* **92**, 211301 (2004) [arXiv:astro-ph/0312134].

- [17] M. Kleban, K. Sigurdson and I. Swanson, “Cosmic 21-cm Fluctuations as a Probe of Fundamental Physics,” JCAP **0708**, 009 (2007) [arXiv:hep-th/0703215].
- [18] Y. Mao, M. Tegmark, M. McQuinn, M. Zaldarriaga and O. Zahn, “How accurately can 21 cm tomography constrain cosmology?,” Phys. Rev. D **78**, 023529 (2008) [arXiv:0802.1710 [astro-ph]].
- [19] B. Freivogel and M. Kleban, “A Conformal Field Theory for Eternal Inflation,” to appear.
- [20] G. Hinshaw *et al.* [WMAP Collaboration], Astrophys. J. Suppl. **180**, 225 (2009) [arXiv:0803.0732 [astro-ph]].